

Reaction–diffusion models of within-feather pigmentation patterning

Richard O. Prum* and Scott Williamson

Department of Ecology and Evolutionary Biology, and Natural History Museum, University of Kansas, Lawrence, KS 66045-2454, USA

Feathers are complex, branched keratin structures that exhibit a diversity of pigmentation patterns. Feather pigments are transferred into developing feather keratinocytes from pigment cells that migrate into the tubular feather germ from the dermis. Within-feather pigment patterns are determined by differential pigmentation of keratinocytes within independent barb ridges during feather development. Little is known about the molecular mechanisms that determine which keratinocytes receive pigment. We apply reaction–diffusion models to the growth of within-feather pigment patterns based on a realistic model of feather growth. These models accurately simulate the growth of a diversity of the within-feather pigmentation patterns found in real feathers, including a central patch, a ‘hollow’ central patch, concentric central patches, bars, chevrons, a central circular spot, rows of paired spots, and arrays of offset dots. The models can also simulate the complex transitions between distinct pigmentation patterns among feathers observed in real avian plumages, including transitions from bars to chevrons, bars to paired dots, and bars to arrays of dots. The congruence between the developmental dynamics of the simulated and observed feather patterns indicates that the reaction–diffusion models provide a realistic and accurate description of the determination of pigment pattern within avian feather follicles. The models support the hypothesis that within-feather pigmentation patterning is determined by antagonistic interactions among molecular expression gradients within the tubular follicle and feather germ.

Keywords: feathers; pigmentation; reaction–diffusion models; activator–inhibitor

1. INTRODUCTION

The development of morphological pattern is a central question in biology (Thompson 1942; Portmann 1952; Turing 1952; Meinhardt 1982; Murray 1989; Ball 1998). A general principle of developmental biology is that complex morphological patterns are not specified in exhaustive detail but, rather, are determined by general developmental mechanisms whose outcomes are specified by a limited number of critical parameters. Theoretical models of morphogenesis can often contribute to the elucidation of the developmental mechanisms that determine complex morphological patterns (Ball 1998).

Feathers are excellent examples of complex and diverse biological structures (Lucas & Stettenheim 1972). The structural diversity of feathers is complemented by a substantial diversity in colour and colour patterning (figure 1). Variation in colour within and among feathers contributes, in fundamental ways, to the function of avian plumage in camouflage, thermoregulation, mate choice, and other communication. (Hereafter, feather pigmentation patterning will refer to patterns *within* individual feathers).

The development of avian plumage coloration is extremely complex. The plumage of an individual bird includes many thousands of feathers that can vary extensively in their pigmentation patterns. Correlation in pigmentation patterning among follicles within and among different feather tracts creates distinct plumage patches that produce many species- and sex-specific variations in integumentary appearance (Price & Pavelka 1996). In

many bird species, the feathers grown from individual follicles during different moults differ in feather pigmentation pattern as extensively as any two feathers in the entire plumage. For example, many contour feathers from the same follicles of a male ruff (*Philomachus pugnax*, Scolopacidae) differ dramatically in size, shape and pigmentation patterning between the sexually dimorphic, alternate plumage exhibited on breeding leks and the sexually monomorphic, basic plumage that moults in for the non-breeding season.

Feather colours can be structural, pigmentary, or a combination of both (Lucas & Stettenheim 1972; Fox 1976; Brush 1978; Prum 1999a). The most common feather pigments are melanins and carotenoids (Brush 1978). Melanins, in particular, produce the most complex and well-defined feather pigment patterns. The models presented here focus on melanin patterning within feathers, but they may also describe the mechanisms of morphogenesis of other pigmentary and structural colour patterns.

Mechanisms of feather pigment pattern development are obscured by the complexity of feather growth itself. Essentially, a feather is a tubular integumentary appendage that grows at its base from a feather follicle—a cylindrical invagination of the epidermis (Lucas & Stettenheim 1972; Prum 1999b). The barbs of a feather grow from longitudinally compartmentalized sections of the tubular epidermis of the developing feather germ. The unique branched structure of the barbs and rachis of a pennaceous feather develop by helical growth of barb ridges around the tubular feather germ (figure 2; Lucas & Stettenheim 1972; Prum 1999b). Generally, new barb ridges originate at the new barb locus on the posterior side of

* Author for correspondence (prum@ku.edu).

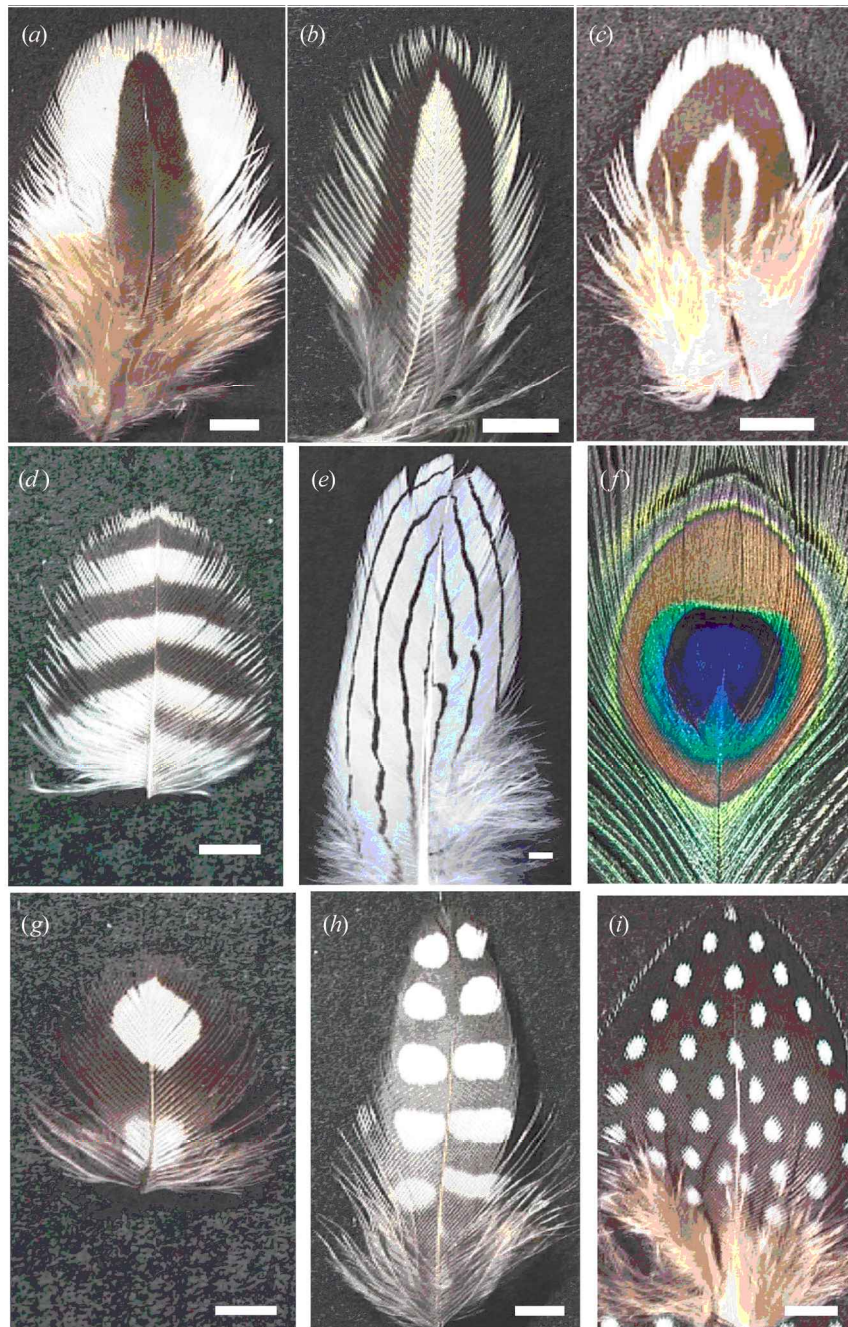


Figure 1. Examples of the diversity of within-feather pigmentation patterns: (a) central pigment patch (*Leucosarcia melanoleuca*, Columbidae, KU 80434); (b) 'hollow' central patch with a non-pigmented centre (*Picus squamatus*, Picidae, KU 43829); (c) concentric central patches (*Crypturellus tataupa*, Tinamidae, KU 87964); (d) bars (*Phloeceastes guatemalensis*, Picidae, KU 51192); (e) chevrons (*Lophura nycthemera*, Phasianidae); (f) a circular central spot or 'eye' (*Pavo cristatus*, Phasianidae); (g) pair of distal and proximal circular central spots (*Chrysocolaptes lucidus*, Picidae, KU 48841); (h) rows of laterally paired spots (*Cyrtonyx montezumae*, Phasianidae, KU103297); (i) array of offset dots (*Guttera pucherani*, Numididae, KU 37708). Scale bars, 5 mm.

the follicle, and then grow helically around the follicle to fuse together to form the rachis ridge at the anterior margin of the follicle (figure 2). When they reach the anterior side of the feather germ, subsequent bar ridges then fuse to the rachis ridge to create the branched form. Pinnaceous feathers only obtain their mature planar form after emerging from the cylindrical feather sheath. At that time, the barb ridges expand their angle with respect to the rachis to form the vane (Prum & Williamson 2001).

Feather melanins come from melanocytes of neural crest origin (Lecoin *et al.* 1998). These melanocytes

migrate into the tubular epidermis of the developing feather germ from the dermal pulp in the centre of the feather germ (Strong 1902; Greite 1934; Watterson 1942). These melanocytes extend pseudopodia among the epidermal cells of the barb ridges and transfer fully developed melanosomes to the developing feather keratinocytes (figure 3; Strong 1902; Greite 1934; Watterson 1942; Lucas & Stettenheim 1972). Melanosomes are actively taken into the keratinocytes by phagocytosis (Greite 1934; Watterson 1942; Lucas & Stettenheim 1972; Jimbow & Sigiyaama 1998; Sharlow *et al.* 2000), and

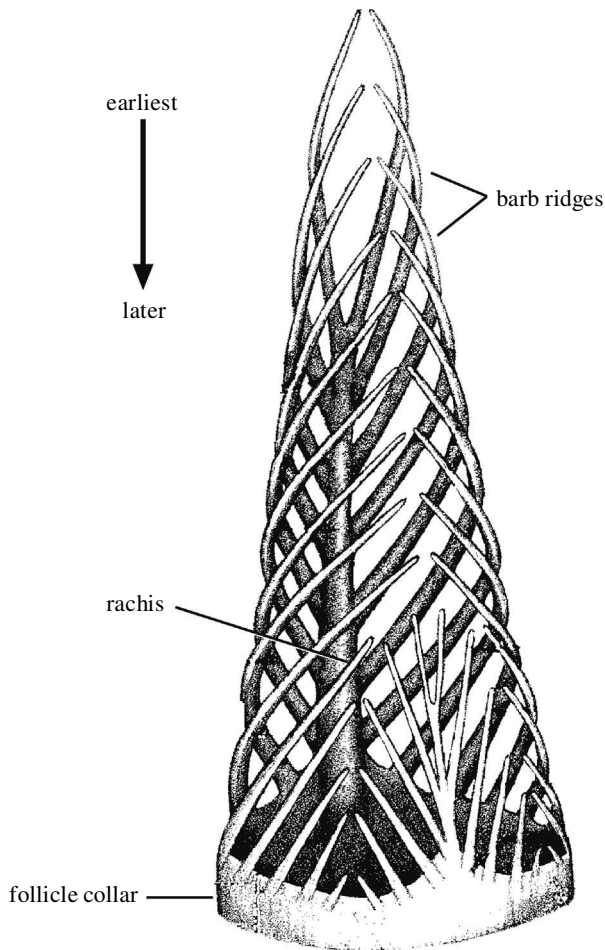


Figure 2. Diagram of helical growth of barb ridges within a developing feather germ, from Lucas & Stettenheim (1972). The branched structure of the rachis and barbs of a pennaceous feather develop by helical growth of barb ridges around the cylindrical feather follicle. New barb ridges originate at the new barb locus (or loci) on the posterior margin of the follicle and grow helically toward the anterior margin to fuse to the rachis. A pennaceous feather obtains its planar vane only after emergence from the cylindrical feather sheath.

are incorporated into the keratin of that cell as it completes its development and dies.

Feather pigmentation patterns are incredibly diverse (figure 1). Except for the trivial cases of feathers with a differentially pigmented tip, we know of no feather pigmentation patterns that are created *exclusively* by the differential coloration of *entire barbs* (see figure 8a). Virtually all feather pigment patterns require differential pigmentation of keratinocytes *within* individual barb ridges. Furthermore, virtually all feather pigment pattern elements are created by the differential pigmentation of *multiple* barb ridges that grow independently within the follicle. Thus, barb ridge identity itself has essentially no role in determining feather pigment pattern formation. Rather, patterns of melanosome transfer are determined by some mechanism that operates over space and time, around the cylindrical feather germ during feather growth. Furthermore, since it is the distal barbules (those extending toward the distal tip of the feather) of a pennaceous barb that reach over the obverse, or outer, surface of the vane to

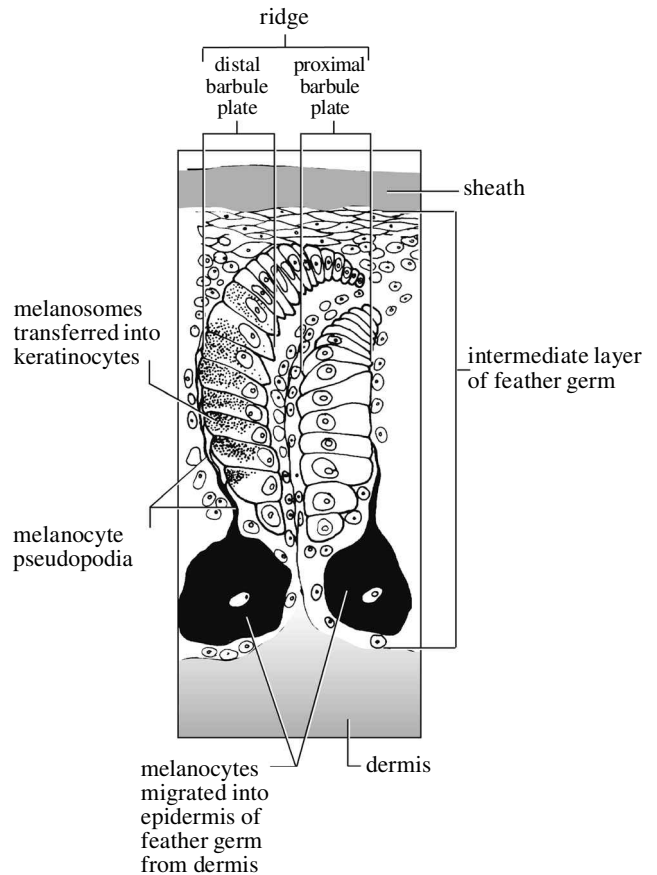


Figure 3. Transfer of melanosomes from melanocytes into the keratinocytes of a developing feather barb ridge, based on Strong (1902). Interactions between melanocyte pseudopodia and feather keratinocytes determine differential transfer of melanosomes into feather keratinocytes. In this example, melanocytes are transferred into keratinocytes of the distal barbule plate (left) but not to the proximal barbule plate (right) that comprise a single barb ridge. At this early stage of barb ridge development, the ramus of the barb has yet to form.

connect with the proximal barbules, melanin is frequently more densely deposited in the distal barbules of a barb (figure 3). So, the mechanisms determining differential melanin uptake by feather keratinocytes also operate within a single barb ridge among closely adjacent cells.

Currently, there is no generalized theory for the developmental determination of feather pigmentation patterns. Hardesty (1933) made an outstanding early attempt. Almost 20 years before Alan Turing (1952), Hardesty used the reinforcing interactions among wave equations to model the formation of the patterned arrays of dots of a guineafowl feather. However, her theory was based on an erroneous model of feather growth (Prum & Williamson 2001). Other attempts have been made to explain the growth of horizontally barred patterns with temporal physiological cycles (e.g. Willier 1941; Rawles 1960), but these physiologically proximate models were not generalizable to any other patterns.

The challenge in conceptualizing feather pigment pattern development is to reconcile the tubular nature of the feather follicle and germ (Lucas & Stettenheim 1972; Prum 1999b) and the helical growth of pennaceous feather barbs (Prum & Williamson 2001) with the final planar

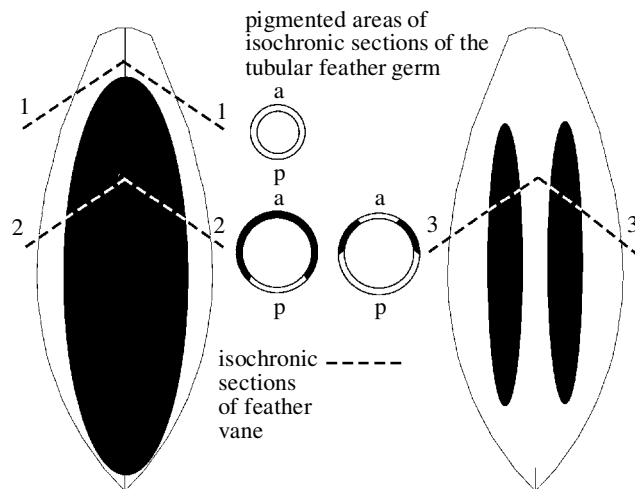


Figure 4. A schematic representation of the distribution of melanosome uptake by keratinocytes in the tubular feather germ epidermis during the growth of different feather patterns. The chevron-shaped isochronic sections (dashed lines) of a feather vane are produced at the same time in a circular isochronic cross section of the tubular feather germ (circles). During the growth of the distal tip of a feather with the central pigment patch (Isochrone 1), the tubular feather germ is entirely non-pigmented. During the growth of a more basal portion of a vane, with a pigmented central patch and a non-pigmented margin (Isochrone 2), the keratinocytes in the anterior three-quarters of the tubular feather germ receive melanosomes while the keratinocytes of the posterior quarter do not. During the growth of a lateral pair of pigment patches (Isochrone 3), melanosomes are transferred only to keratinocytes in two lateral regions of an isochronic section of the feather germ. a, anterior; p, posterior.

form of the mature pennaceous feather. Because of the uniform linear growth rate of barb ridges, the angle of helical growth of barb ridges within the feather germ, and the expansion of the angle between the barbs and rachis at the emergence of the mature feather from the sheath, an isochronic section of cells from the tubular feather follicle (i.e. all originating at the same time) is not a horizontal section of the feather vane, but a chevron-shaped section of the vane centred on the rachis (figure 4; Prum & Williamson 2001). Furthermore, as a consequence of the formation of new barb ridges on the posterior margin of the follicle and helical growth toward the dorsal margin, barb ridge cells originating on the posterior surface of the follicle collar become the peripheral margins of the vane, whereas barb ridge cells on the dorsal surface of the feather follicle contribute to the central portion of the vane. Thus, differential pigmentation patterns within the planar feather vane result from the differential pigment uptake by keratinocytes over time within the tubular feather germ. In figure 4, a simple schematic illustrates how the spatial distribution of pigment uptake within the tubular feather germ can contribute to different pigment patterns in the mature feather vanes.

We apply reaction–diffusion models of pigmentation patterning to developing feather germs. First devised by Turing (1952) and subsequently advanced by others (e.g. Meinhardt 1982; Murray 1989), reaction–diffusion equa-

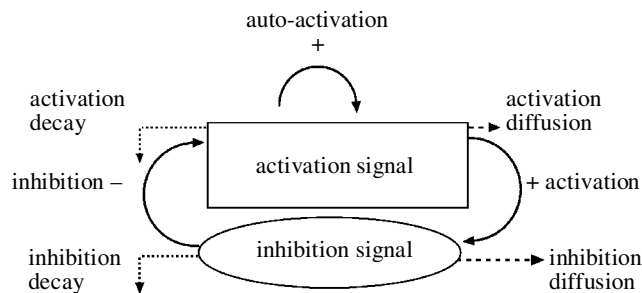


Figure 5. Schematic of a generalized reaction–diffusion system (equations (2.1a) and (2.1b)) based on Ball (1998). The activating signal reinforces its own production and the production of the inhibitory signal, which inhibits the production of the activating signal. Both activating and inhibitory signals diffuse and decay over time. See § 2 for details.

tions (figure 5) have been used to model pattern formation in many developmental systems, and have been applied specifically to a number of questions in integumentary pigment patterning (Gierer & Meinhardt 1972; Meinhardt 1982, 1995, 1998; Murray 1989; Kondo & Asai 1995; Price & Pavelka 1996; Meinhardt & Gierer 2000). Here, we simulated pennaceous feather growth using a six-parameter computer model that was developed to study the growth of feather shape (Prum & Williamson 2001). We apply various formulations of reaction–diffusion mathematics to simulate different classes of feather pigmentation patterns, transition among feathers with different patterns, and two ‘counterfactual’ patterns which apparently do not exist among real feathers. The realism of the simulations, and the predictions and implications of the models are then discussed.

2. MATERIAL AND METHODS

Feather growth was simulated with a six-parameter mathematical model of feather growth (Prum & Williamson 2001) using MATLAB 5, a versatile and widely used matrix algebra program (<http://www.mathworks.com/>). The feather growth model parameters include: (i) barb and rachis ridge growth rate, (ii) angle of helical barb ridge growth, (iii) initial barb ridge number, (iv) new barb ridge addition rate, (v) barb ridge diameter, and (vi) the angle of barb ramus expansion following emergence from the sheath (Prum & Williamson 2001). The feather growth model simulates the size and positions of the barb and rachis ridges, and the total size of the follicle collar for series of time intervals throughout the growth of a pennaceous feather. All simulations were conducted using a single idealized feather shape with the same parameter values (table 1). The effect of variation in feather shape on feather pigmentation patterns will be investigated in future research.

The pigmentation of the developing feather barb keratinocytes was modelled as a temporal series of spatial fields—the ring-shaped follicle collar at the base of the feather germ—in which morphogenesis signals interact and propagate through time. Melanin transfer was determined by a critical threshold magnitude of an activating morphogenetic stimulus at the place and time of keratinocyte origin in the follicle collar. Negative patterns with non-pigmented pattern elements on a generally pigmented vane were modelled by assigning the absence of melanin transfer to a critical threshold of magnitude. All feather pigmen-

Table 1. Parameter values for the within-feather pigmentation pattern simulations illustrated in figures 5–7.^a

| figure | equation | growth | D_a | D_b | D_c | b_a | b_b | r_a | r_b | r_c | threshold | s_x | s_t | p | a_{or} | a_{on} | b_0 | c_{or} | c_{on} |
|--------|---------------------|--------|--------|-------|-------|-------|--------|-------|-------|-------|-----------|-------|-------|-----|-------------------|----------|-------|----------|----------|
| 5a | 2.1a ₃ b | rachis | 0.03 | 0.25 | | 0.004 | 0.0014 | 0.01 | 0.015 | | 0.7 | 14 | 9 | | 0.5 | 0.3 | 1 | | |
| 5b | 2.1a ₁ b | rachis | 0.0025 | 0.2 | | 0.008 | 0 | 0.01 | 0.015 | | 1.5 | 14 | 9 | | 0.5 | 0.3 | 1 | | |
| 5c | 2.1a ₁ b | rachis | 0.0085 | 0.2 | | 0.008 | 0 | 0.01 | 0.015 | | 1.5 | 8 | 9 | | 0.5 | 0.3 | 1 | | |
| 5d | 2.1a ₁ b | margin | 0.04 | 0.04 | | 0.001 | 0 | 0.02 | 0.01 | | 0.7 | 14 | 20 | | 0.5 | 0.3 | 1 | | |
| 5e | 2.2a ₃ b | margin | 0.003 | 0 | | 0.008 | 0.004 | 0.08 | 0.007 | | 0.3 | 18 | 10 | 1.3 | 1 | 0 | 1 | | |
| 5f | 2.3a–c | margin | 0.05 | 0.04 | 0.006 | 0.03 | 0 | 0.008 | 0.003 | 0.003 | 1 | 8 | 5 | | 0.25 | 0.07 | 1 | 0.4 | 0.85 |
| 5g | 2.3a–c | margin | 0.05 | 0.04 | 0.02 | 0.03 | 0 | 0.15 | 0.008 | 0.003 | 1 | 8 | 3 | | 1 | 0.7 | 1 | 0.65 | 1 |
| 5h | 2.3a–c | margin | 0.02 | 0.4 | 0.14 | 0.05 | 0 | 0.02 | 0.01 | 0.005 | 1.55 | 8 | 3.5 | | 0.75 ^b | 0.75 | 1 | 1 | 1 |
| 5i | 2.3a–c | margin | 0.008 | 0.4 | 0.006 | 0.03 | 0 | 0.02 | 0.01 | 0.002 | 1 | 20 | 15 | | 0.25 | 0.6 | 1 | 0.5 | 1.2 |
| 6bL | 2.2a ₃ b | margin | 0.003 | 0 | | 0.08 | 0.06 | 0.08 | 0.007 | | 0.3 | 18 | 10 | 1 | 1 | 0 | 1 | | |
| 6bC | 2.2a ₃ b | margin | 0.003 | 0 | | 0.008 | 0.05 | 0.08 | 0.007 | | 0.3 | 18 | 10 | 1.3 | 1 | 0 | 1 | | |
| 6bR | 2.2a ₃ b | margin | 0.003 | 0 | | 0.008 | 0.004 | 0.08 | 0.007 | | 0.3 | 18 | 10 | 1.3 | 1 | 0 | 1 | | |
| 6eL | 2.3a–c | margin | 0.02 | 0.4 | 0.04 | 0.05 | 0 | 0.02 | 0.01 | 0.005 | 1.55 | 8 | 3.5 | | 0.75 ^b | 0.75 | 1 | 1 | 1 |
| 6eC | 2.3a–c | margin | 0.02 | 0.4 | 0.04 | 0.05 | 0 | 0.02 | 0.01 | 0.005 | 1.55 | 8 | 3.5 | | 0.75 ^b | 0.75 | 1 | 1 | 1 |
| 6eR | 2.3a–c | margin | 0.02 | 0.4 | 0.14 | 0.05 | 0 | 0.02 | 0.01 | 0.005 | 1.55 | 8 | 3.5 | | 0.75 | 0.75 | 1 | 1 | 1 |
| 6gL | 2.3a–c | margin | 0.02 | 0.4 | 0.1 | 0.05 | 0 | 0.02 | 0.01 | 0.002 | 1 | 20 | 15 | | 1.325 | 0.75 | 1 | 1 | 1 |
| 6gC | 2.3a–c | margin | 0.013 | 0.4 | 0.11 | 0.05 | 0 | 0.02 | 0.01 | 0.002 | 1 | 20 | 15 | | 1.325 | 0.75 | 1 | 1 | 1 |
| 6gR | 2.3a–c | margin | 0.013 | 0.4 | 0.12 | 0.05 | 0 | 0.02 | 0.01 | 0.002 | 1 | 20 | 15 | | 1.325 | 0.75 | 1 | 1 | 1 |
| 7b | 2.2a ₃ b | margin | 0.003 | 0 | | 0.008 | 0.04 | 0.08 | 0.007 | | 0.15 | 14 | 10 | 1.3 | 1 | 0 | 1 | | |

^a Equations (2.1)–(2.3) and parameters are described in § 2. The five columns on the right give the initial concentrations of the activators and inhibitors (a_0, b_0, c_0). For a and c , the initial concentrations are specified as a_{or} and c_{or} at the rachis, and a_{on} and c_{on} at all other positions. Parameters for the feather growth simulations (Prum & Williamson 2001): absolute growth rate, $m = 0.18$; angle of helical growth, $\theta = 6^\circ$; initial barb number, 8; barb ridge addition parameters, $w = 1, q = 0.0001$; barb ridge diameter, $d = 0.15$; length, $l = 80$; angle of barb ramus expansion, $\beta = 39^\circ$. R, right; L, left; C, centre.

^b For these simulations, different initial concentrations of the activator were specified for the fourth and fifth of the six compartments of each side of the feather germ. $a_{04} = 1.1, a_{05} = 0.85$.

tation patterns were simulated in MATLAB 5 using the discrete forms of one-dimensional reaction–diffusion equations devised by Meinhardt & Klingler (1987) and Meinhardt (1998) to model integumental patterning in molluscs. In their simplest form, these reaction–diffusion models hypothesize a chemical morphogen—an activator—that stimulates both its own production and the production of a second compound—an inhibitor—which inhibits the production of the activator (figure 5). Differential diffusion rates, background production rates, and decay rates of the activator and the inhibitor can result in both spatial and temporal periodicity in activator concentration. If a morphogenetic event (e.g. melanin transfer) is linked to a critical value of morphogen concentration, the result could be spatial or temporal patterns in morphology. Alternative versions of the models hypothesize an activator whose concentration is determined by a limiting substrate (Meinhardt & Klingler 1987; Meinhardt 1998).

The field width at any time was determined by the simulated circumference of the follicle collar and feather germ at that time, measured by numbers of discrete ‘cells’. The field size is proportional to the width of an isochronic section of the feather vane (Prum & Williamson 2001). The expansion and shrinkage of the field in response to the changing circumference of the feather germ were simulated in three ways. In posterior growth, cells were added and deleted at the posterior margin of the feather germ (which becomes the margins of two sides of the vane). In stretching growth, cells were added and deleted at random positions within the field. In anterior growth, cells were added and deleted from the field at the anterior margin of the feather germ adjacent to the rachis (which becomes the centre of the vane). New cells received the morphogen concentrations of their nearest neighbours. The scale of the field relative to the scale of the feather was determined by two parameters: s_x is the number of cells per unit distance in the feather, and s_t is the number of time steps of pattern generation per time step of feather growth. With few exceptions (figure 8), the morphogenic field was modelled with diffusing conditions at the rachis and reflecting boundary conditions at the new barb locus (where the left and right sides of the follicle meet on the ventral side of the feather germ).

The simplest feather pigmentation patterns (figure 6*a–d*) were simulated with an activator–inhibitor model represented by the following system of equations:

$$\frac{\partial a}{\partial t} = r_a \left(\frac{a^2}{b} + b_a \right) - r_a a + D_a \frac{\partial^2 a}{\partial x^2} \quad (2.1a)$$

$$\frac{\partial b}{\partial t} = r_a a^2 + b_b - r_b b + D_b \frac{\partial^2 b}{\partial x^2} \quad (2.1b)$$

where $a(x, t)$ and $b(x, t)$ represent the activator and inhibitor concentrations, respectively (eqn 2.1 in Meinhardt 1998). b_a and b_b are the independent production rates of the activator and inhibitor, r_a and r_b are the decay rates, and D_a and D_b are the diffusion rates, respectively. The first term on the right hand side of equation (2.1*a*) is multiplied by r_a so that the total activator production and decay are, on average, equivalent over the life of the feather. Unless otherwise stated, all parameters retained constant values across space and time. When the inhibitor diffusion rate is greater than seven times that of the activator diffusion rate ($D_b \gg D_a$), the result is spatially stable peaks in activator concentration (Meinhardt 1998).

Additional pigmentation patterns (figures 6*e* and 7*b*) were simulated according to an activator–substrate depletion model.

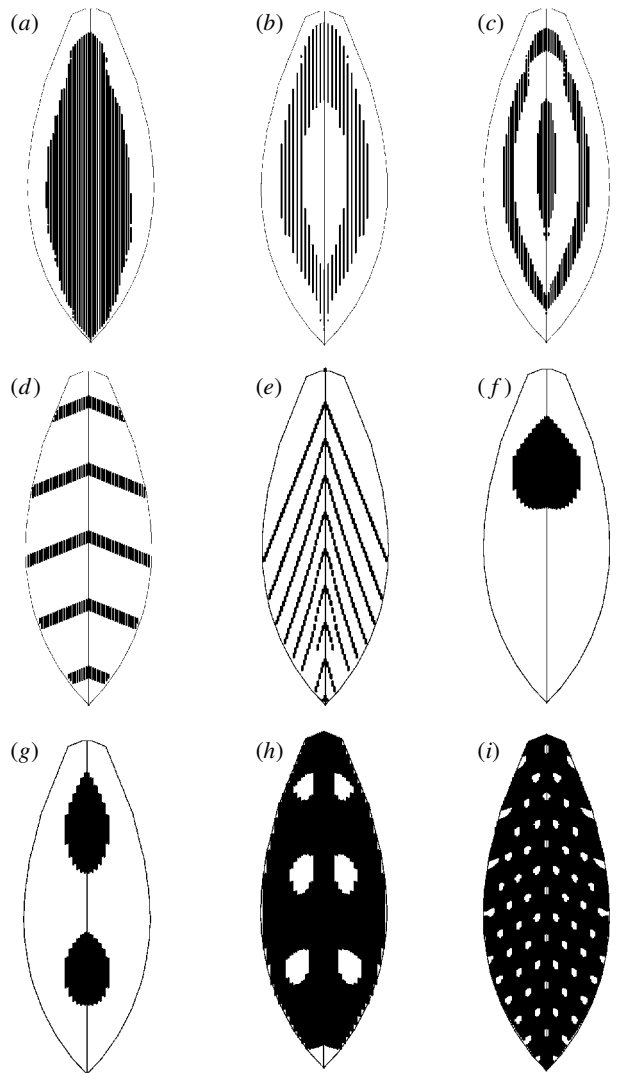


Figure 6. Reaction–diffusion simulations of within-feather pigmentation patterns: (a) central pigment patch; (b) ‘hollow’ central patch with a non-pigmented centre; (c) concentric central patches; (d) bars; (e) chevrons; (f) a circular central spot or ‘eye’; (g) distal and proximal pair of circular central spots; (h) rows of laterally paired spots; (i) array of offset dots.

Here, the antagonistic interaction is due to the depletion of the substrate by the activator:

$$\frac{\partial a}{\partial t} = r_a b (a^2 + b_a) - r_a a + D_a \frac{\partial^2 a}{\partial x^2} \quad (2.2a)$$

$$\frac{\partial b}{\partial t} = b_b - r_a b (a^2 + b_a) - r_b b + D_b \frac{\partial^2 b}{\partial x^2} \quad (2.2b)$$

Again, $a(x, t)$ is the activator concentration, and $b(x, t)$ is the substrate concentration (eqn 2.4 in Meinhardt 1998). Here, b_b is the independent background production rate of the substrate. In the substrate models (equations (2.2*a,b*)), the background production rate of the substrate, b_b , at the rachis can be multiplied by an additional factor, p . When $p > 1$, the cells at the rachis become excitable at a higher frequency than the surrounding cells, creating a pacemaker region (Meinhardt 1998).

The reaction–diffusion systems based on two interacting signals (equations (2.1*a,b*)) can produce spatial periodicity or temporal periodicity depending on the values of various parameters. However, more complex patterns require overlaying spatially

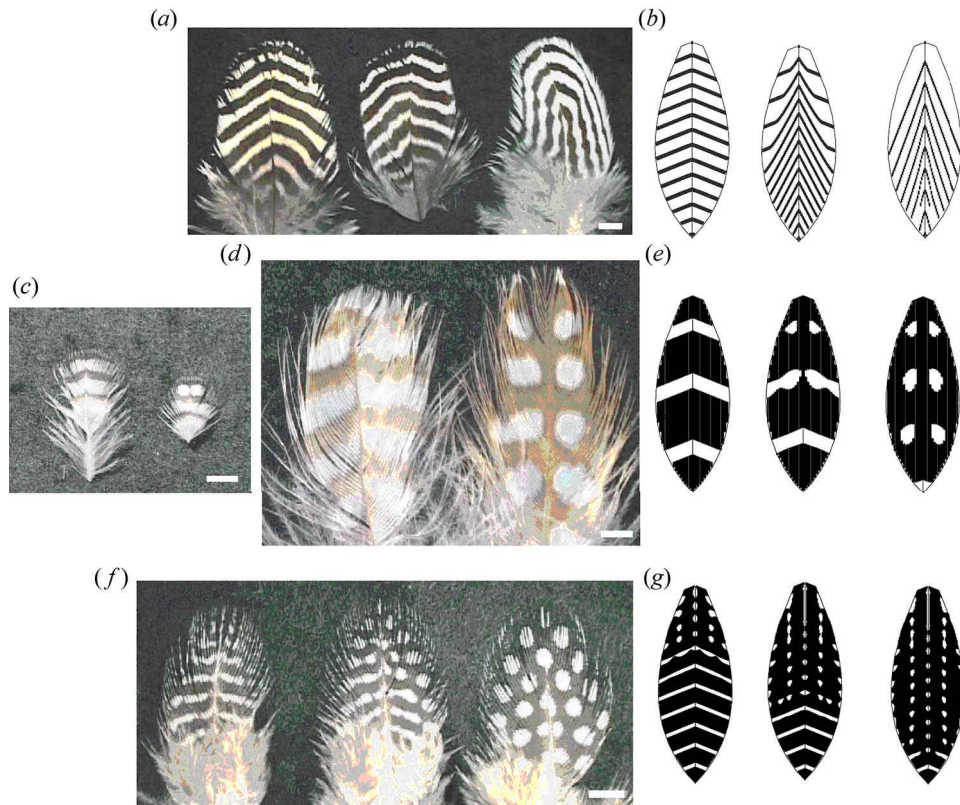


Figure 7. Real and simulated pigment pattern transitions among feathers from the same tract: (a) transition from bars to chevrons (*Eupodotis atra etoschae*, Otidae, KU 86156); (b) simulated transition from bars to chevrons; (c) transition from bars to distal pair of lateral dots (*Pytilia melba*, Estrildidae, KU REM 795); (d) transition from bars to a series of laterally paired dots (*Spilornis cheela panayensis*, KU 43654); (e) simulated transition from bars to distal pair of dots to a series of laterally paired dots; (f) transition from bars to an array of dots (*Numida meleagris reichenowi*, Numididae, KU 29479); (g) simulated transition from bars to an array of dots.

and temporally periodic patterns. These more complex patterns (figures 6*f–i* and 7*c,e*) were simulated by an activator–two inhibitor model, in which one inhibitor causes stable patterns and the other causes periodic patterns:

$$\frac{\partial a}{\partial t} = \frac{r_a}{c} \left(\frac{a^2}{b} + b_a \right) - r_a a + D_a \frac{\partial^2 a}{\partial x^2} \quad (2.3a)$$

$$\frac{\partial b}{\partial t} = \frac{r_b a^2}{c} - r_b b + D_b \frac{\partial^2 b}{\partial x^2} \quad (2.3b)$$

$$\frac{\partial c}{\partial t} = r_c a - r_c c + D_c \frac{\partial^2 c}{\partial x^2} \quad (2.3c)$$

In this model, r_c and D_c are the decay rate and diffusion rate of the second inhibitor, $c(x, t)$, which inhibits both the activator and the first inhibitor (eqn 5.3 in Meinhardt 1998). With appropriate parameter values, interactions between the spatial and temporal periodicities induced by the two inhibitors can create complex oscillating patterns.

Parameter values that successfully simulated the various classes of feather pigmentation patterns were identified by exploration of the parameter spaces of the different reaction–diffusion equations. (Essentially, this trial and error method was a form of artificial selection with non-random mutation; our understanding of the equations provided some predictive insight into the relationship between parameter values and outcomes, but the complexity of the models also created unexpected effects on pattern.) Initial morphogen concentrations were specified at the beginning of each simulation. Generally, initial concentrations were either uniform across the entire field, or uniform except

for a different concentration at the anterior-most cell nearest to the rachis. Parameter values for each illustrated simulation can be found in table 1.

These models hypothesize that the pigmentation fate of a keratinocyte is determined within a single isochronic section of the feather germ. However, melanosome transfer actually occurs over a period during feather development corresponding to an undetermined length of the growing feather germ. Until the molecular signals underlying the differentiation of melanin receiving and non-receiving keratinocytes are understood, it is not possible to know how accurate our assumption of isochronic fate determination really is.

Although each simulated feather is composed of a series of barbules attached to the rachis, the illustrations are simplified to show only the outline of the pennaceous feather vane.

3. RESULTS

(a) Simulations of within-feather patterns

Through a general survey of a large diversity of avian specimens from almost all extant orders we identified a number of general classes of feather pigmentation patterns (figure 1).

The simplest feather pigmentation pattern is a central patch (figure 1*a*). The growth of a central pigment patch can be simulated accurately with differential diffusion rates of activating and inhibitory signals (figure 6*a*). Another common pattern with a narrow, pigmented edge on the distal half of the vane only (e.g. silver laced Wyan-

dotte chickens), can be simulated with the same conditions as a complete central patch but with an order of magnitude lower background rate of inhibitor production (not illustrated). More complex patterns featuring a 'hollow' patch with a non-pigmented central area (figure 1*b*) and a set of concentric central patches (figure 1*c*) can also be simulated by assuming a different activation diffusion rate, a different scale (s_x), and anterior field growth (figure 6*b,c*).

Barred feather patterns are common in many avian orders (figures 1*d* and 7*a*), and can be accurately simulated by assuming similar activation and inhibition diffusion rates but with a higher rate of activation decay (figure 6*d*).

More complex pigment patterns require simultaneous spatial and temporal pattern differentiation. For example, chevrons (figures 1*e* and 7*a*) can be simulated with an activator–substrate depletion model using a higher substrate production rate at a 'pacemaker' zone near the rachis (figure 6*e*).

The 'eye' of a male peacock tail feather (*Pavo*, Phasianidae) (figure 1*f*) is a single central pattern element that, unlike a simpler central patch (figure 1*a*), is not determined by the vane width. Although the peacock eye is produced by structural colours, with complex variations in hue (Durrer 1962), the hue and shape of the pattern is ultimately determined by the distribution of melanin granules in the barbules of the developing barb ridges that have the same developmental origin. The outline of a peacock 'eye' spot can be simulated with the addition of a second inhibitory signal that inhibits both the activating and primary inhibitory signals (figure 6*f*). Two, additional, closely related patterns were accidentally generated in early attempts to simulate the growth of the peacock 'eyes', but we then identified these patterns in several real feathers. The first of these patterns—a distal and proximal pair of central spots (figure 6*g*)—was subsequently identified in the contour feathers of the woodpecker *Chrysocolaptes lucidus* (Picidae) (figure 1*g*). A second pattern—a single distal dot with a lateral pair of proximal dots—was also identified in another woodpecker species (not illustrated). In both cases, the proximal pattern elements on these feathers were not visible in the plumage, because the basal portions of the feather vanes were covered by the tips of the neighbouring (rostral) feathers within the feather tract.

Another complex pattern—a series of laterally paired dots—is found in numerous avian families (e.g. Accipitridae, Phasianidae, Picidae, Estrildidae; figure 1*h*). The growth of rows of paired dots can also be simulated with a two-inhibitor system (figure 6*h*).

Among the most complex of all feather pigmentation patterns are the arrays of offset white dots on the melanin-pigmented vanes of guineafowl feathers (Numididae) (figure 1*i*). This class of patterns can be simulated by hypothesizing an oscillating interaction between spatial and temporal inhibition by a pair of inhibitory signals (figure 6*i*). A common anomaly in the simulated guineafowl patterns shows a striking congruence with developmental anomalies observed in real guineafowl feathers. Hardesty (1933) observed that neighbouring dots within an isochronic (i.e. chevron-shaped) row of dots on a guineafowl contour feather occasionally unite into a

single, larger spot. Our simulations commonly produced similar horizontal fusions (not illustrated). By incrementally increasing the threshold of morphogenesis in a series of these simulations, we demonstrated that these fused dots are actually merged independent activator peaks (not illustrated). Varying the threshold of morphogenesis in this manner also creates changes in dot size that closely match variations among various guineafowl species (e.g. figures 1*i* and 7*f*; simulations not illustrated).

(b) *Simulations of pattern transitions among feathers*

Many bird plumages exhibit striking transitions between different feather pigmentation patterns among feathers over the body. Although the two endpoint patterns are completely distinct, transitional feathers in between exhibit intermediate patterns that bridge the disparate endpoints. These transitional pigment patterns are unlikely to be determined by a large series of distinct mechanisms. Rather, transitions between different patterns are probably determined by a common, general mechanism with an underlying variation in parameter values.

Reaction–diffusion models can accurately simulate the general dynamics of several major classes of pattern transition observed in real bird plumages. For example, *Eupodotis* bustards (Otididae) show a gradation in pattern from bars on their backs to chevrons on their upper sides (figure 7*a*). This pattern transition can be simulated with an activator–substrate system (equations (2.2*a,b*)) that uses a 'pacemaker' to increase the substrate production rate at the rachis (figure 7*b*). Many diverse species exhibit a transition from bars to lateral pairs of dots that typically begins at the tip of the feathers (figure 7*c,d*). This pattern transition can be simulated with a two-inhibitor system and additional variation in the initial conditions (figure 7*e*). Lastly, in certain guineafowl (e.g. *Numida meleagris reichenowi*), the breast feathers intergrade from horizontal bars on the throat to hexagonal arrays of offset dots on the belly (figure 7*f*). Feathers in the transitional zone exhibit distal dots with basal bars (figure 7*f*, centre). We simulated the growth of a similar pattern transition by using a temporal gradation in the imposition of a second inhibitory signal (figure 7*g*). Although it is possible to create specific models for the determination of each type of plumage pattern, the reaction–diffusion models provide a plausible general mechanisms for the observed, complex transitions between distinct patterns within the plumage of an individual bird.

(c) *Simulation of unknown pigment patterns*

Simulations of unknown feather pigment patterns can help identify developmental conditions that do not, or cannot, exist in real feather follicles. Simulations of 'counterfactual' feathers may contribute additional predictions into the probable mechanisms of feather pigment pattern determination.

As mentioned above, we simulated a pattern of differential 'whole-barb' pigmentation by growing a feather with a repeated series of ten pigmented barbs followed by ten non-pigmented barbs on both sides of the vane (figure 8*a*). This pattern is not determined by reaction–diffusion dynamics, but uses barb ridge identity to specify whether any specific keratinocyte within them will receive melanin.

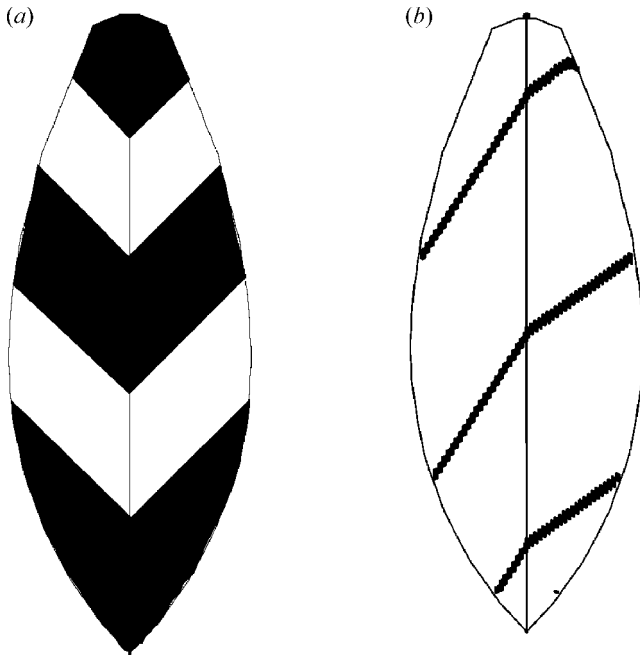


Figure 8. Simulated 'counterfactual' pigmentation patterns that are not known among real feathers: (a) a pattern produced by pigmenting *entire* barb ridges one colour or another, specifically an alternating pattern of ten pigmented bars and ten non-pigmented on each side of the vane; (b) bar sinister pattern produced by an activating peak travelling entirely around the cylindrical feather germ during growth (like the stripes on a barber's pole). The angular break in the bar at the rachis is due to the angular expansion of barb ridges after emergence from the cylindrical sheath (Prum & Williamson 2001).

There are trivial examples of a simple distal tip pattern that could be explained by a simple barb-identity patterning rule (i.e. pigment only in the first few barbs on each side of the vane; e.g. *Oxyruncus cristatus*, Cotingidae; *Melospiza melodia*, Emberizidae). However, these simple patterns could also be explained by a simple spatio-temporally-based patterning process. We know of no feather pigment patterns or pattern element based solely on variation in pigment deposition *among* entire barb ridges. Virtually all feather pigment patterns require variation in pigmentation *within* barbs. Apparently, barb ridge identity has no role in the determination of feather pigmentation patterning.

In addition, we identified a second theoretically plausible feather pigment pattern that apparently does not occur among real feathers. Propagation of an activation peak completely around the cylindrical feather germ (like a stripe on a barber's pole) would result in a bar sinister pattern in a mature feather (figure 8b). The bar sinister pattern apparently does not exist among real avian feathers, implying that pigmentation patterning signals cannot propagate across the new barb ridge locus on the posterior margin of the tubular feather germ. The apparent absence of such patterns suggests that the tubular developmental field of the feather germ behaves as a linear field, delimited by the posterior new barb locus, which is only incidentally circular.

4. DISCUSSION

(a) *Realism of the models*

These reaction–diffusion models provide the first generalized theory of the growth of feather pigment patterns. Various versions of the models can accurately simulate the growth of many major classes of feather melanin pigmentation. In general, the congruence between simulated and real feather pigment patterns supports the realism and accuracy of the models. However, we identified several instances in which the details of the behaviour of the simulations matches the dynamics of real feather patterns in a manner that strongly supports the realism of the models.

First, the reaction–diffusion models can simulate the complex transitions between distinct feather pigmentation patterns (figure 7). Such transitions in pigment pattern among feathers are a common feature of avian plumages. It is possible (but unlikely) that such transitions are determined by a large series of distinct mechanisms. In contrast, these reaction–diffusion models can simulate some of the major classes of these pattern transitions with simple changes in one or a few parameters, and hence, in a more parsimonious and realistic manner.

Second, pigmentation patterns in some bird feathers exhibit anomalous, unpredictable deviations in pattern (i.e. fused guineafowl dots; Hardesty (1933)). Because these pattern anomalies are repeated identically in the subsequent feathers grown from the same follicles (Hardesty 1933), they are likely to be caused by variations in conditions that are intrinsic to individual follicles and that are determined early in the development of follicle identity. In our simulations of guineafowl feathers, we found that small variations in parameter values could reproduce identical pattern anomalies.

Third, artificial selection on simulated pigment patterns produced some of the same detailed dynamics observed as a consequence of natural or sexual selection on pigment patterns in real bird feathers. We identified two instances in which selection on simulated and real pigment patterns resulted in correlated expression of the same, *non-functional* pattern elements. In our attempts to simulate the peacock 'eyespot', we identified a broad set of parameter conditions that would produce the desired circular spot in the middle of the distal portion of the vane, but these conditions also created additional, undesired basal pattern elements—either a single basal dot (figure 6g) or a lateral pair of double basal dots (not illustrated)—that are not present in the target peacock feather pattern. Subsequently, however, we discovered both of these patterns in contour feathers of two independent species of woodpeckers (Picidae) (figure 1g). In both woodpecker species, these correlated basal pattern elements were completely obscured from view by the overlying tips of the adjacent, rostral feathers, creating a plumage patch with a field of distinct distal circles. Thus, in both the artificial selection of our simulations and in the evolutionary history of these woodpeckers, selection for a single, circular, distal spot led to the correlated expression of the same, *non-functional* basal pattern elements. These results document that the reaction–diffusion simulations of the growth of feather pigmentation patterning are similar in striking detail to the developmental and evolutionary dynamics of real feather patterns.

Meinhardt & Klingler (1987) and Meinhardt (1998) developed the reaction–diffusion models applied here to simulate the growth of mollusc shell pigment patterns. Our simulation of feather pigment patterns documents that biologically very distinct patterns can be successfully modelled with the same mathematics.

Our simulations provide support for the realism of reaction–diffusion models in feathers, specifically, and other developmental systems, in general (Ball 1998). However, these models also extend the application of reaction–diffusion equations in integumentary patterning to new size scales and complexities. Previous applications of reaction–diffusion equations to integumentary patterning have typically modelled the entire integument as a single morphogenetic field (Meinhardt & Klingler 1987; Murray 1989; Kondo & Asai 1995; Price & Pavelka 1996; Meinhardt 1998). In contrast, feather follicles are small (often less than 5 mm in diameter), numerous (more than 5000 per individual), and can grow highly differentiated and patterned feathers through successive moults for the entire life of the bird.

These models could be further explored and expanded to simulate even more patterns. There is substantial additional diversity in feather pigmentation patterns, including the enormous variety of patterns in pheasants (especially the Argus pheasant, *Argusianus*), and the camouflage patterns in owls (Strigiformes), nightjars (Caprimulgidae), and others that are created by variations in the density of pigment deposition of black eumelanin and red–brown phaeomelanins. Further, there is the subject of how feather shape itself influences feather pigmentation patterning. For example, we have observed that feather pigment patterns are distorted in specific, predictable ways by changes in feather shape, such as in asymmetrical remiges. These systems would provide additional challenges to the models.

(b) *Testable predictions*

The next important step will be to test these models with investigations of the molecular and cellular mechanisms of the development of feather pigmentation patterns. Fortunately, these reaction–diffusion models generate many testable hypotheses. First, these results imply that feather pigmentation patterning is determined by interactions of chemical gradients operating within the cylindrical feather follicle and germ. Further, our results indicate that this morphogenetic field is not truly cylindrical. The apparent absence of feather pigment patterns that require signal propagation across the new barb locus on the posterior margin of the follicle (e.g. the bar sinister or barber's pole pattern; figure 8b) indicates that this is not mechanistically plausible. Thus, these results predict that feather pigmentation patterning is based on a fundamental anterior–posterior gradient in expression of pigment pattern formation genes in the two sides of the follicle and feather germ. This gradient is not strictly anterior–posterior in orientation, however. In flight feathers with an asymmetrical vane, the new barb locus is laterally displaced within the cylindrical feather follicle away toward the lateral margin (Strong 1902; Lucas & Stettenheim 1972; Prum & Williamson 2001), but pigment patterning within asymmetrical feathers remains coherent within both the left and right sides of the vane.

Second, these models imply that antagonistic interactions between activating and inhibiting signals are fundamental to the mechanism of feather pigment pattern determination. The original reaction–diffusion models hypothesized specific activator and inhibitor molecules diffusing through an essentially uniform medium (e.g. Turing 1952; Kondo & Asai 1995). In contrast, we propose that the models actually describe the interactions between morphogenic signalling pathways among the discrete developing keratinocytes of the cylindrical feather germ. In determining what developmental outcome to express, keratinocytes within the barb ridges of the growing feather both generate and respond to extracellular morphogenetic signals. We hypothesize that the sum of these activating and inhibiting signals among the field of feather keratinocytes converges on the differential equations used in the reaction–diffusion systems.

Third, given the discontinuity of the two sides of the follicle at the posterior new barb locus, these models can easily be expanded to create different pigment patterns for the left and right sides of the vane. There are relatively few feathers that have entirely independent pigment patterns on the left and right sides of the vane. For example, the sides of the breast of the Montezuma quail, *Cyrtonyx montezumae* (Odonotophoridae) have a few such feathers at the border between two distinctly patterned patches of breast feathers within a single feather tract. The patterns on each side of the vane are completely distinct, but they match the patterns found in the plumage patches adjacent to that side of the follicle. Such natural pigmentation pattern 'chimerae' present an opportunity to test the interactions between the mechanisms specifying the differential pigmentation patterns among and within follicles. Apparently, as the pigment pattern identities of neighbouring plumage patches are specified early in development, it appears that some follicles on the border of these two distinct plumage fields actually specify different pattern identities on each side of the follicle.

(c) *Supporting evidence from feather development and genetics*

Congruence between a theoretical model of morphogenesis and organic forms is not by itself sufficient to conclude that the model is an accurate depiction of a biological process (Niklas 1994). It is also important to observe whether the mechanisms hypothesized by the model are biologically realistic. In this instance, our simulations are based on the most recent understanding of how branched feathers grow (Prum & Williamson 2001), but there is little recent research on the development of feather pigmentation patterns. However, there is some classical experimental evidence in support of the hypothesis that feather pigmentation patterns are determined by molecular gradients within the follicle.

Lillie & Juhn (1932) performed experiments on the effects of sex hormones on the development of feather pigmentation patterning in a chicken breed with sexual dimorphic plumage. Their interpretations of their results led to an erroneous theory of feather development based on differential rates of barb ridge growth and the 'con-crescence' hypothesis of rachis formation (reviewed in Prum & Williamson 2001). However, their experimental disruptions of feather pigment patterning did document

an anterior–posterior gradient in response to hormones. Brief, high concentration pulses of hormones selectively disrupted pigmentation of barb ridges in the posterior half of the feather germ, and thus affected patterning of the distal tips of the barbs that form the margins of the vane. In contrast, low concentrations of hormones for longer periods selectively disrupted pigmentation of barbs in the anterior half of the feather germ, and thus affected patterning of the basal portions of barbs that form the central areas of the feather vane. These response gradients do not reflect differential growth rates (Prum & Williamson 2001), as hypothesized by Lillie & Juhn (1932). Although the details of the observed responses are difficult to interpret, the results of Lillie & Juhn (1932) do support the role of anterior–posterior molecular gradients within the feather germ in the development of pigmentation feather patterns.

Lillie & Wang (1941) and Cohen & 'Espinasse (1961) performed a series of experiments transplanting portions of the dermal papillae (with or without the epidermal collar) between regenerating follicles from pigmented and non-pigmented feather tracts. Although the results of these experiments were highly variable and showed substantial artefacts, Lillie & Wang (1941) and Cohen & 'Espinasse (1961) confirm that distal and ventral portions of the papilla generally determine the patterns of the central and marginal portions to the vane.

There are numerous classical studies of experimental transfer of ectoderm among non-pigmented, pigmented, and pigment-patterned breeds of chicken (reviewed in Rawles 1960). However, these experiments are quite difficult to interpret since there are many different ways that any given mutation can influence the ultimate pigmentation of a feather, from melanocyte origin, migration and melanogenesis to final melanosome transfer.

Classical genetic studies have identified and genetically mapped some of the genes associated with within-feather pigmentation patterns of chickens (referred to as secondary pigment patterns in a review by Smyth (1990)). These studies have identified combinations of 17 alleles at six different loci that determine ten, autosomal within-feather pigment patterning phenotypes in domestic chickens (*Gallus gallus*) (Smyth 1990). However, a large number of additional pigment pattern modifier genes have yet to be identified (Smyth 1990). These data document that different feather patterns in chickens can be transformed by one, or several, genetic changes.

(d) *Evolution of avian pigmentation patterns*

The evolution of pigmentation patterning within and among feathers has proceeded by natural and sexual selection on the capacities of the follicle and feather germ to grow appropriately pigmented feathers in the appropriate places and times over the life of the bird. These models provide the first explicit predictions about the types of developmental changes required for the evolution of novel feather pigment patterns. Similarly, Price & Pavelka (1996) used reaction–diffusion equations to model the development of avian plumage patches, such as wing bars and crown stripes, and to make predictions about the nature of convergent evolution in plumage pattern elements. Recent research by Theron *et al.* (2001) on the genetic and molecular basis of melanism in Caribbean popu-

lations of bananaquit (*Coereba flaveola*) further demonstrate the future promise of molecular and developmental studies of the evolution of plumage colour patterning. Future research on the molecular mechanisms behind the feather pigment pattern development will help us understand how plumage colours have evolved for cryptic, social, and sexual functions.

A simple comparative survey of feather pigmentation patterning demonstrates that avian clades vary tremendously in their capacity to grow complexly patterned feathers. For example, many galliform families have feathers with extremely complex pigment patterns. In contrast, other families and orders may entirely lack complex feather patterns (e.g. Pelecaniformes). Further, specific pattern elements appear to predominate within specific clades (e.g. arrays of dots in Numididae, or pairs of spots in Estrildidae). Those feather pigment patterns that require the most complex molecular mechanisms (i.e. two interacting inhibitory signals) appear to show the most restricted taxonomic distributions.

Thus, the capacity to grow complex feather pigment patterns has its own evolutionary history. Various feather pigment patterns have convergently evolved many times. Characterization of the molecular and cellular mechanisms of feather pigmentation pattern will allow us to discover whether convergent patterns in different avian clades use the same or distinct molecular mechanisms. Furthermore, some clades are apparently constrained in their capacity to evolve feather pigment pattern complexity. Such phylogenetic constraints are apparently independent of social selection on plumage because even some clades known for brilliant plumage and intense sexual selection lack almost all within-feather pigment patterning (e.g. Pipridae).

The authors thank Rodolfo Torres and Estela Gavosto for their mathematical inspiration, and for introducing us to Meinhardt's (1998) *Algorithmic beauty of sea shells*. The manuscript was improved by comments from Alan Brush, Matthew Harris, Peter Stettenheim, and several anonymous reviewers. The research was supported by grants to R.O.P. from the University of Kansas Graduate Research Fund and the National Science Foundation (DBI-0078376). Feather specimens were provided by the Division of Ornithology of the University of Kansas Natural History Museum and Biodiversity Research Center (KU). Chris Sheil helped prepare figure 3.

REFERENCES

- Ball, P. 1998 *The self-made tapestry: pattern formation in nature*. Oxford University Press.
- Brush, A. H. 1978 Avian pigmentation. In *Chemical zoology* (ed. A. H. Brush), pp. 141–164. New York: Academic Press.
- Cohen, J. & 'Espinasse, P. G. 1961 On the normal and abnormal development of the feather. *J. Embryol. Exp. Morphol.* **9**, 223–251.
- Durrer, H. 1962 Schillerfarben beim Pfau (*Pavo cristatus* L.). *Verh. Naturf. Ges. Basel* **73**, 204–224.
- Fox, D. L. 1976 *Animal biochromes and structural colors*. University of California Press.
- Gierer, A. & Meinhardt, H. 1972 A theory of biological pattern formation. *Kybernetik* **12**, 30–39.
- Greite, W. 1934 Die Strukturbildung der Vogelfeder und ihre Pigmentierung durch Melanine. *Z. wiss. Zool.* **145**, 284–334.
- Hardesty, M. 1933 The feather of guineafowl and a mathemat-

- ical theory of individual feather patterns. *J. Exp. Zool.* **66**, 53–86.
- Jimbow, K. & Sigiyma, S. 1998 Melanosomal translocation and transfer. In *The pigmentary system: physiology and pathophysiology* (ed. J. J. Nordlund, R. E. Boissy, V. J. Hearing, R. A. King & J. P. Ortonne), pp. 107–114. New York: Oxford University Press.
- Kondo, S. & Asai, R. 1995 A reaction–diffusion wave on the skin of a marine fish. *Nature* **376**, 765–768.
- Lecoin, L., Lahav, R., Dupin, E. & Le Douarin, N. 1998 Development of melanocytes from neural crest progenitors. In *molecular basis of epithelial appendage morphogenesis* (ed. C. M. Chuong), Georgetown, TX: R. G. Landes Co.
- Lillie, F. R. & Juhn, M. 1932 The physiology of development of feathers. I. Growth-rate and pattern in individual feathers. *Physiol. Zool.* **5**, 124–184.
- Lillie, F. R. & Wang, H. 1941 Physiology of development of the feather. V. Experimental morphogenesis. *Physiol. Zool.* **14**, 103–133.
- Lucas, A. M. & Stettenheim, P. R. 1972 *Avian anatomy—integument*. Washington, DC: US Department of Agriculture.
- Meinhardt, H. 1982 *Models of biological pattern formation*. London: Academic Press.
- Meinhardt, H. 1995 Dynamics of stripe formation. *Nature* **376**, 722–723.
- Meinhardt, H. 1998 *The algorithmic beauty of sea shells*. Berlin: Springer.
- Meinhardt, H. & Gierer, A. 2000 Pattern formation by local self-activation and lateral inhibition. *BioEssays* **22**, 753–760.
- Meinhardt, H. & Klingler, M. 1987 A model for pattern formation on the shells of mollusks. *J. Theor. Biol.* **126**, 63–69.
- Murray, J. D. 1989 *Mathematical biology*. Berlin: Springer.
- Niklas, K. J. 1994 Simulation of organic shape: the roles of phenomenology and mechanism. *J. Morphol.* **219**, 243–246.
- Portmann, A. 1952 *Animal forms and patterns: a study of the appearance of animals*. London: Faber & Faber.
- Price, T. & Pavelka, M. 1996 Evolution of a colour pattern: history, development, and selection. *J. Evol. Biol.* **9**, 451–470.
- Prum, R. O. 1999a The anatomy and physics of avian structural coloration. In *Proc. 22nd Int. Ornithol. Congr.* (ed. N. J. Adams & R. H. Slotow), pp. 1633–1653. Johannesburg: BirdLife South Africa.
- Prum, R. O. 1999b Development and evolutionary origin of feathers. *J. Exp. Zool. (Mol. Devl Evol.)* **285**, 291–306.
- Prum, R. O. & Williamson, S. 2001 A theory of the growth and evolution of feather shape. *J. Exp. Zool. (Mol. Devl Evol.)* **291**, 30–57.
- Rawles, M. E. 1960 The integumentary system. In *Biology and comparative physiology of birds* (ed. A. J. Marshall), pp. 189–240. New York: Academic Press.
- Sharlow, E. R., Paine, C. S., Babiariz, L., Eisinger, M., Shapiro, S. & Seiberg, M. 2000 The protease-activated receptor-2 upregulates keratinocyte phagocytosis. *J. Cell Sci.* **113**, 3093–3101.
- Smyth Jr, J. R. 1990 Genetics of plumage, skin, and eye pigmentation in chickens. In *Poultry breeding and genetics* (ed. R. D. Crawford), pp. 109–167. Amsterdam: Elsevier.
- Strong, R. M. 1902 The development of color in the definitive feather. *Bull. Mus. Comp. Zool.* **40**, 147–185.
- Theron, E., Hawkins, K., Bermingham, E., Ricklefs, R. E. & Mundy, N. I. 2001 The molecular basis of an avian plumage polymorphism in the wild: a *melanocortin-1-receptor* point mutation is perfectly associated with the melanic plumage morph of the bananaquit, *Coereba flaveola*. *Curr. Biol.* **11**, 550–557.
- Thompson, D. A. W. 1942 *On growth and form*. Cambridge University Press.
- Turing, A. M. 1952 The chemical basis of morphogenesis. *Phil. Trans. R. Soc. Lond.* **237**, 37–72.
- Watterson, R. L. 1942 The morphogenesis of down feathers with special reference to the developmental history of melanophores. *Physiol. Zool.* **15**, 234–259.
- Willier, B. H. 1941 An analysis of feather color pattern produced by grafting melanophores during embryonic development. *Am. Nat.* **75**, 136–146.

As this paper exceeds the maximum length normally permitted, the authors have agreed to contribute to production costs.